PROCEEDINGS, 42nd Workshop on Geothermal Reservoir Engineering
Stanford University, Stanford, California, February 13-15, 2017
SGP-TR-212

Numerical Modelling of Geothermal Reservoirs with Multiple Pore Media

Musa D. ALIYU[1], Hua-Peng CHEN[1], Ouahid HARIRECHE[2], and Colin D. HILLS[1]

[1]Department of Engineering Science, University of Greenwich, Medway Campus, Kent, UK

[2]Department of Civil Engineering, Islamic University of Medina, Medina, Saudi Arabia

m.d.aliyu@greenwich.ac.uk, h.chen@greenwich.ac.uk, c.d.hills@greenwich.ac.uk

Keywords: dual-porosity model, triple porosity-permeability, deep geothermal reservoirs, multiple pore media, graben formation

ABSTRACT

Geothermal energy is clean, renewable, sustainable, and is independent of weather, place, and time. To harness this energy form requires drilling two or more wells in a crystalline formation to create a reservoir. However, field experiments are expensive to perform, but with the aid of modelling, the reservoir behaviour during exploration/exploitation can adequately be predicted. The dual-porosity modelling approach has been widely adopted in describing most naturally fractured geothermal reservoirs with two contiguous (i.e. matrix and fractures), but there are still some shortcomings when employing the dual-porosity model to represent deep geothermal reservoirs with multiple pore media, such as reservoirs with natural fractures, micro-fractures, and faults. In this study, the concept of triple porosity-permeability is proposed to represent reservoir heterogeneity better in naturally fractured and faulted reservoirs. The triple porosity-permeability modelling approach proposed in this study describes flow through naturally fractured reservoirs with different petrophysical properties, among which porosity and permeability are of primary interest. The media resides in a formation that is formed by three distinct continua of matrix, fractures, and faults, such as the graben formation of the Soultz geothermal system. In the Soultz graben, the series of fractures are interconnected with large faults, and fluid and heat are transmitted via these structures. The study develops a numerical model based on finite element methods for analysing coupled heat transport and fluid flow responses of the Soultz (France) deep heterogeneous geothermal reservoir. The model proposed here can reflect transient temperature distributions during a long-term simulation of 30 years, as well as pressure distribution among multiple pore media. Further, the model also considers density and viscosity variation in deep geological formations during production.

1. INTRODUCTION

Naturally fractured media have been the object of multiple studies for more than fifty years. To explain their behaviour in different fields such as groundwater, geothermal and petroleum reservoirs, several models have been created with inherent difficulties to capture realistic models of fractured media because of the partial ignorance about the dimensions, spatial distribution, and interconnections of the fractured network (Suirez-Arriaga 2002). Numerical models are one of the most valuable predictive tools available for managing subsurface resources in reservoir engineering. These models are employed to test or refine various conceptual models, estimate thermal, hydraulic, chemical, and mechanical parameters, and, most importantly for geothermal resource management, predicting how the reservoir might respond to changes in exploitation and environment. Numerous models have been successfully developed in geothermal reservoirs; however, the application of numerical models in multiple pore media is more problematic. Multiple pore media are, in most cases, heterogeneous. Thus, they are dominated by primary (matrix), secondary, (fractures) or tertiary (faults or micro-fractures) porosity and may exhibit hierarchical permeability structures or flow paths.

Zimmerman et al. (1993) developed a dual-porosity model for a single-phase fluid flow in a fractured/porous media using a lumped parameter approach for the matrix block. Lim & Aziz (1995) derived a matrix-fracture transfer shape factors for dual-porosity simulation of naturally fractured reservoirs by combining analytical solutions of pressure diffusion for various flow geometries. Choi et al. (1997) applied the Forchheimer equation to model a dual-porosity/dual-permeability model of a reservoir and compared the results with those obtained from the Darcian-flow. Bower & Zyvoloski (1997) extended the stress solution of the FEHM code to the dual porosity capability to determine the hydraulic conductivity of the fracture system. Also, modifications were made to the couple hydrologic, thermal, and mechanical behaviour of the fracture systems. Ranjbar & Hassanzadeh (2011) developed a semi-analytical, dual-porosity model and used a fine-grid, single-porosity numerical model for verifications. Nie et al. (2012) developed a semi-analytical model to analyse a dual porosity and dual permeability flow model of horizontal well production in a naturally fractured reservoir. Austria & Sullivan (2015) carried out a sensitivity analysis to determine when to employ a dual porosity model over single porosity models in modelling geothermal systems. Aliyu et al. (2016) studied the effect of extraction well placement on geothermal energy efficiency using the dual porosity approach. In summary, extensive work has been done on this model and is available in the following literature (Altmann et al. 2014; Kolditz 1995a; Kolditz 1995b; Wang et al. 2015; Mohan et al. 2015; Izadi & Elsworth 2015).

The aim of this work is to introduce some numerical models of geothermal reservoirs supported by existing data of the Soultz geothermal system concerning what could happen in a triple porosity-permeability regime at a full scale, representing the interaction between three different continua in deep subsurface media. The triple porosity-permeability modelling approach proposed in this study describes flow through naturally fractured reservoirs with different petrophysical properties, among which porosity and permeability are of primary interest. The media resides in a formation that is formed by three distinct continua of matrix, fractures, and faults, such as the graben formation of the Soultz geothermal system (Schumacher 2002; Pribnow & Clauser 2000). In the Soultz graben, the series of fractures are interconnected with large faults (Baria et al. 1999; Jain et al. 2015), and fluid and heat are transmitted via these structures.

2. TRIPLE POROSITY-PERMEABILITY MODEL FOR THE FRACTURED POROUS RESERVOIR

The model of triple porosity-permeability accommodates transport from a well within a matrix into fractures and faults. The fluid and heat transport models are developed for this triple porosity-permeability system with combined conservation equations for mass and momentum to define the field equations. The following assumptions are made for the equations:

- The geothermal reservoir is a fractured porous medium containing faults, fractures, and matrix; each medium is homogenous, isotropic, and linear elastic.
- A single fluid phase is considered with temperature dependent density, dynamic viscosity, heat capacity, and thermal conductivity.

The transient flow of mass for the model is given as

$$\begin{aligned} &\rho_L S_j \frac{\partial P_j}{\partial t} + \nabla \cdot \rho_L v_j = Qm_j \quad (for\, mass) \\ &v_j = -\frac{\kappa_j}{\mu} \nabla P_j \\ &\forall j = m, f, F \end{aligned} \tag{1}$$

The sub index j represents transport in the matrix (m), in the fracture (f) and in the fault (F), respectively. The variables ρ_L is the fluid density, S_j is the linearised storage, and P_j is the fluid pressure, Darcy's velocity v_j, is the source/sink term Qm_j, and κ_j is the permeability.

The transient flow of heat for the model is given as

$$\begin{aligned} &(\rho C_P)_j \frac{\partial T_j}{\partial t} + \rho_L C_{P,L} v_j \cdot \nabla T + \nabla \cdot q_j = Q_j \quad (for\, energy) \\ &(\rho C_P)_j = \phi_S (\rho_L C_{P,L}) + (1-\phi_S) \rho_S C_{P,S} \\ &q_j = -\lambda_j \nabla T \\ &\lambda_j = \phi_s \lambda_s + (1-\phi_s) \lambda_L \end{aligned} \tag{2}$$

The variables ρ and C_P (i.e. $(\rho C_P)_j$) are the effective densities and specific heat capacities, respectively, T_j is the temperature, q_j is the heat flux density, and t is time. Properties, $C_{P,S}$ and $C_{P,L}$ corresponds specific heat capacity of solid and fluid, ρ_s is the solid density, is the heat source/sink term Q_j, λ_j is the effective thermal conductivities, ϕ_s is the solid porosity. The variables λ_s and λ_L are solid and fluid thermal conductivities, respectively.

3. MODEL SET-UP AND IMPLEMENTATION

In this segment, a numerical model of the Soultz lower geothermal reservoir is presented. The finite element method has been used as a framework for implementing the proposed triple-porosity-permeability model. Figure 1 presents the physical model of the reservoir, which is decomposed into a matrix, fractures, faults, and wellbores (Gérard et al. 2006). The reservoir matrix is simulated as a 3-D domain while the fractures and faults are presented as two-dimensional (2-D) boundaries that are interconnected with the surrounding matrix. The wellbores GPK3 (injection well), GPK2 (production well), and GPK4 (production well) are simulated as one-dimensional (1-D) geometry.

3.1 Geometry and mesh of the reservoir

The geometrical dimension of the reservoir considered is 2 x 0.5 x 0.68 km^3. It consists of a complex system with fractures and faults and is located at 4.5 km under the ground level (Genter et al. 2010). It contains a triplet representing an injection well (GPK3) and two production wells (GPK2 and GPK4). The injection well (GPK3) is located at x-y coordinates (1 km, 0.25 km), and each of the production wells is 0.6 km away from the injection well (Genter et al. 2009). The hydrological and thermal properties of the geothermal reservoir are shown in Table 1 (Aliyu & Chen 2016; Guillou-Frottier et al. 2013).

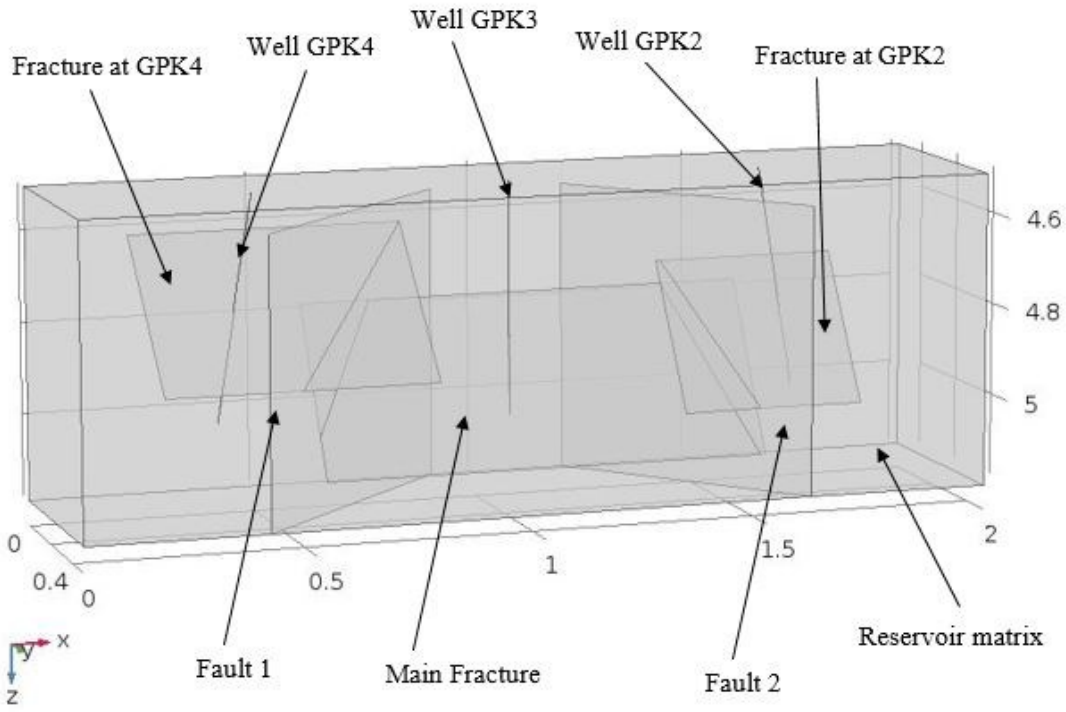

Figure 1: Model geometry and set-up

Figure 2 showed the finite element mesh of the reservoir. The matrix block is discretised using 3-D tetrahedral elements, and the fractures and faults are discretised employing 2-D triangular elements. Furthermore, the wells are discretised using 1-D line elements. The generated mesh consists of 224,084 3-D tetrahedral elements, 10,349 2-D triangular elements, 2,577 1-D line elements, and 71 vertex elements. Due to the complexity of the system, extra fine element sizes are employed for wells, whereas finer element sizes are used for the matrix block; intermediary element sizes are utilised on the fractures and faults with growth rates of 1.35 for the extra fine elements and 1.4 for the finer elements.

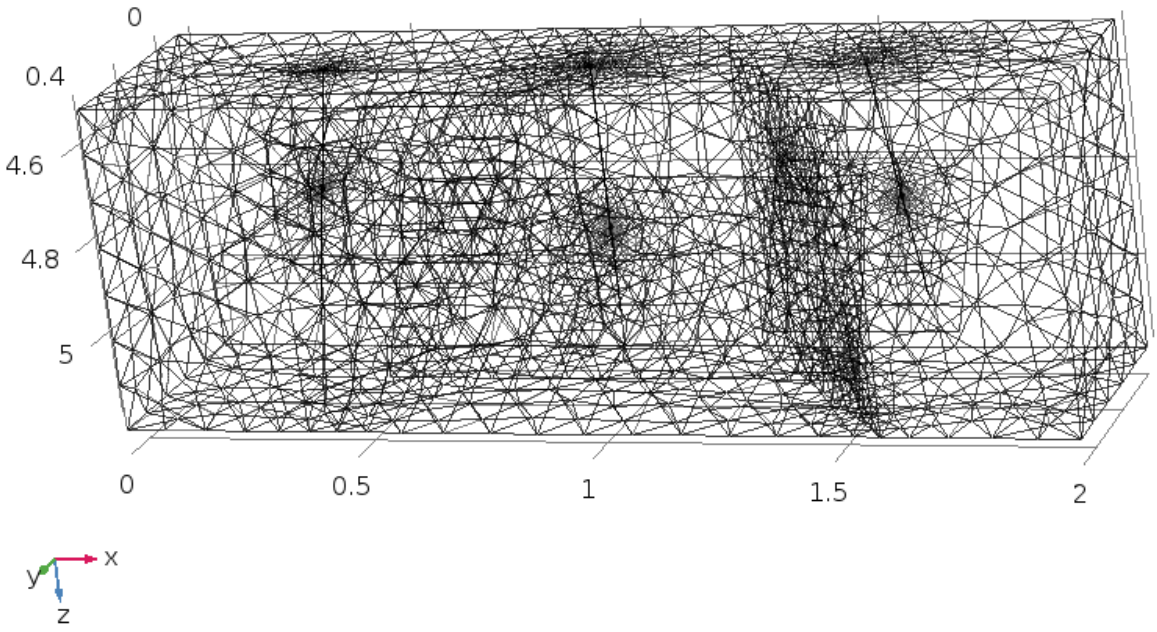

Figure 2: Reservoir model mesh

Table 1: Physical properties attributed to lower reservoir (less permeable granitic basement)

Parameter	Value	Symbol
Matrix		
Porosity (%)	1.0	ϕ
Permeability (mD)	0.001	κ
Thermal conductivity (W/m/K)	3.0	λ_s
Heat capacity (J/kg/K)	850	$C_{\rho,S}$
Density (kg/m^3)	2600	ρ_s
Faults		
Porosity (%)	0.3	ϕ_F
Permeability (mD)	100	κ_F
Thermal conductivity (W/m/K)	2.3	λ_F
Heat capacity (J/kg/K)	850	$C_{\rho,F}$
Density (kg/m^3)	1800	ρ_F
Fractures		
Porosity (%)	0.1	ϕ_f
Permeability (mD)	10	κ_f
Thermal conductivity (W/m/K)	2.5	λ_f
Heat capacity (J/kg/K)	750	$C_{\rho,f}$
Density (kg/m^3)	2000	ρ_f

3.2 Initial and boundary conditions

In this study, the initial temperature is given as

$$T_0(z) = 12°C - 38°C/km \times (-z) \tag{3}$$

where $T_0(z)$ is the initial temperature of the geothermal reservoir, $12°C$ is the assumed value of the surface temperature, $38°C/km$ is the geothermal gradient, and z is depth in kilometres. Also, the initial pressure is assumed to be hydrostatic in the formation.

For the boundary conditions, a Dirichlet boundary condition (BC) of 30°C (injection temperature) is applied at injection well GPK3, whereas for the hydraulic case, 10 MPa (injection pressure) is considered as the Dirichlet BC on the wellbore injection GPK3. Further,

an underpressure BC of -10 MPa is employed on both the production wells GPK2 and GPK4, individually. All other boundaries are considered as adiabatic conditions (insulated) during simulations.

A backwards difference formula (BDF) is used in the COMSOL package to run the long-term simulation for 30 years. The technique holds an advantage of minimising time steps because, in this study, it took only 56 time steps to simulate the 30-year numerical experimentation. The physical memory utilised is 5720 MB, and the virtual memory is 6060 MB.

4. RESULTS AND DISCUSSIONS

In this study, a numerical model of a triple porosity-permeability model is developed using the finite element method for the calculation of coupled transient fluid and heat flow effect in a deep geothermal reservoir. The first sets of the results are shown in Figures 3 and 4, which are the breakthrough curves for both temperature and enthalpy at the production wellhead GPK4, respectively. As seen, the drawdown pattern is similar in both parameters; a decline stage is observed at 6 years, from the beginning of the simulation until the 30-year exploitation period. Thus, for the entire simulation period, there is a drawdown in the production temperature of 30°C, which is equivalent to a decline of 1°C per production year, as shown in the production wellhead temperature of Figure 3. In the case of enthalpy, the drawdown is approximately equal to 133.91 kJ/kg, which is almost equal to a decrease of 4.46 kJ/kg per production year, as presented in Figure 4.

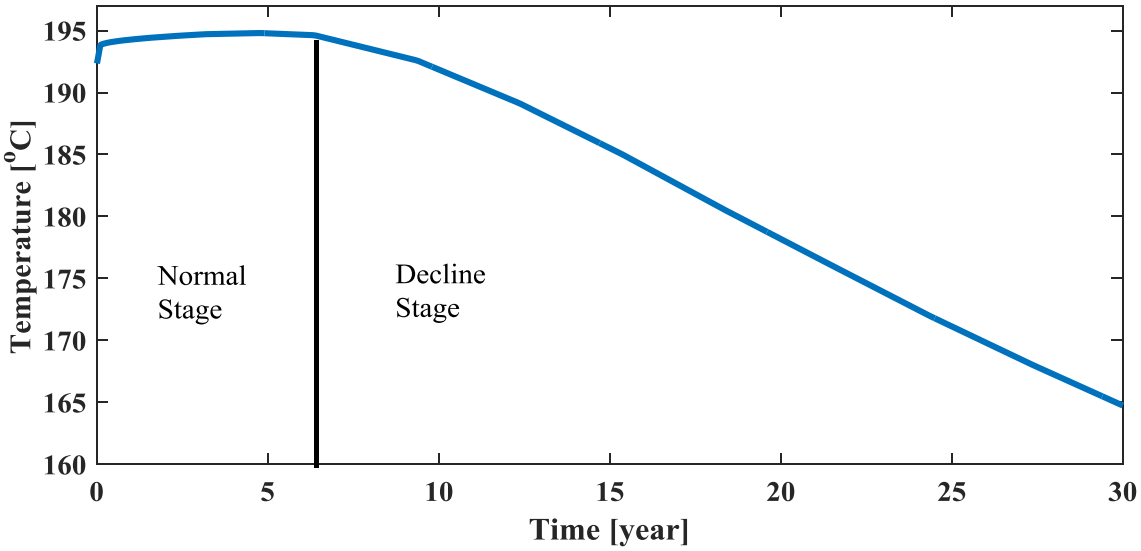

Figure 3: Production temperature at wellhead GPK4

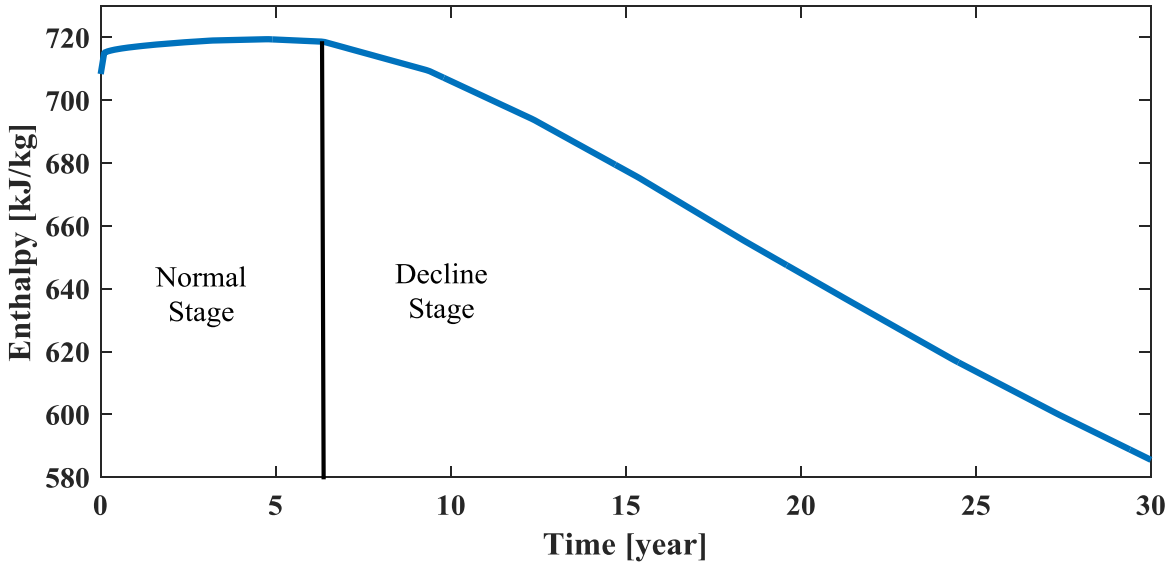

Figure 4: Production enthalpy at GPK4

The second category of the results is presented in Figures 5, 6, 7, and 8, and include the breakthrough curves at the fracture-faults' intersection points for the temperature, pressure, dynamic viscosity, and fluid density. Figure 5 showed the temperature profile at the fracture-faults' intersection points for the 30-year simulation period. As can be seen, there is a drawdown at both points; in both cases, the maximum temperatures obtained are 192.9°C and 193°C at 1.5 and 1.6 years, respectively. The temperature at 30 years' declines to 91°C and 102°C at each intersection point 1 and 2. The reason for this sudden decline in temperature is explained in figure 6, which presents the pressure profile at the intersection points. The pressure increase proves that there is no further fracturing at the points, which confirms no opening for additional heat to flow.

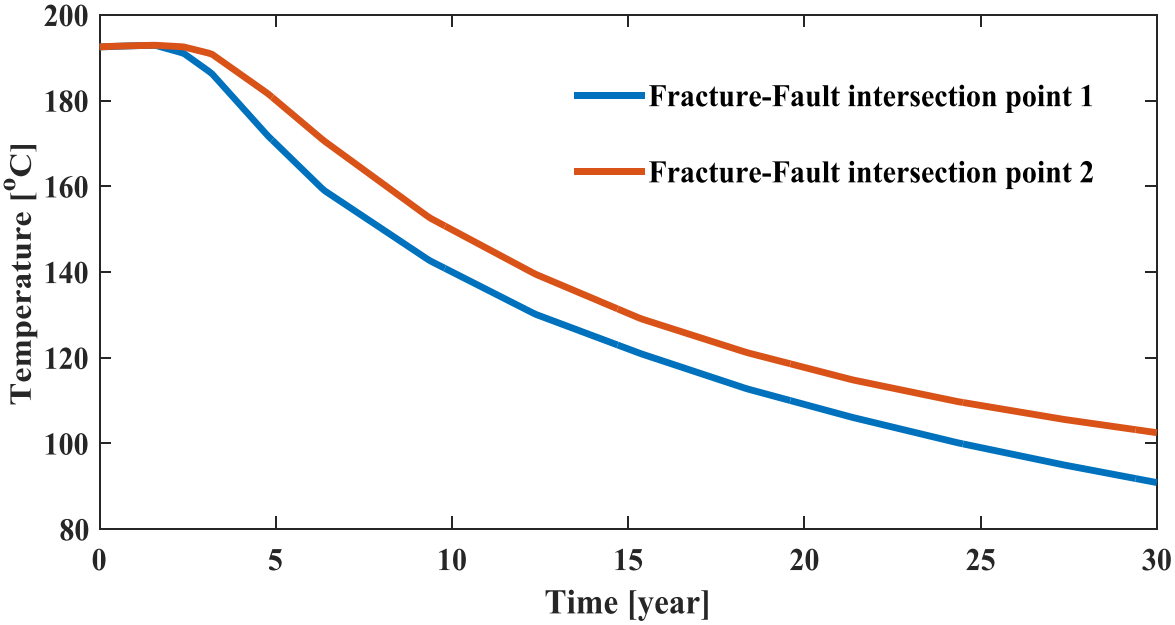

Figure 5: Temperature profile at fracture-fault intersection points

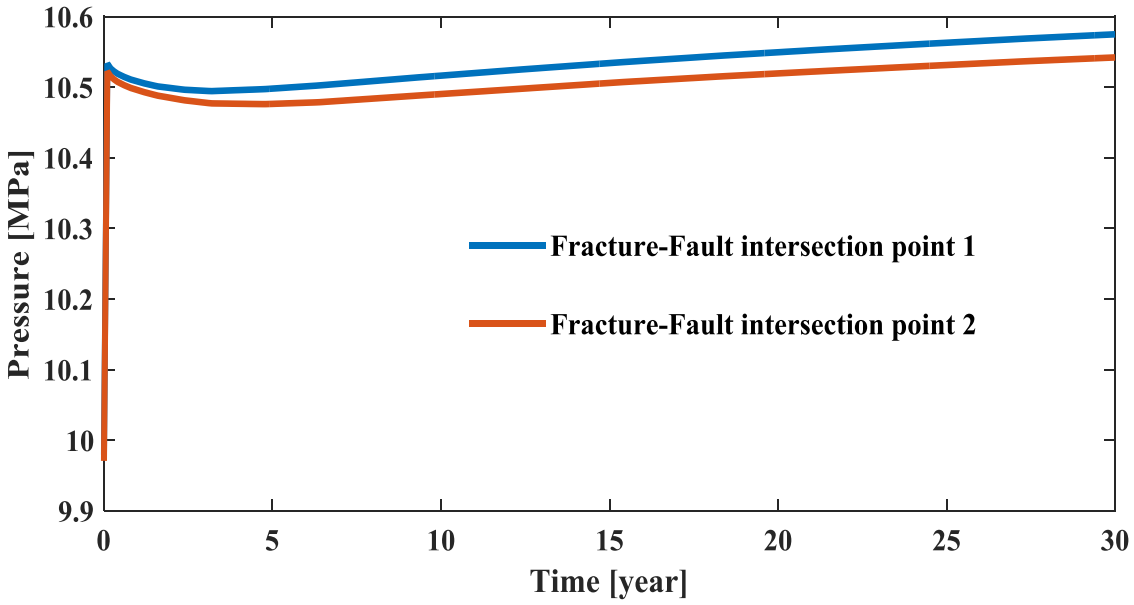

Fig. 6: Pressure profile at fracture-fault intersection points

Figures 7 and 8 show the dynamic viscosity and density breakthrough curves at the fracture-fault intersection points. As seen in the two figures, both parameters increase at the intersection points throughout the simulation period because dynamic viscosity and density are functions of temperature; thus, as the temperature decreases, the viscosity and density of the fluid increase and vice versa.

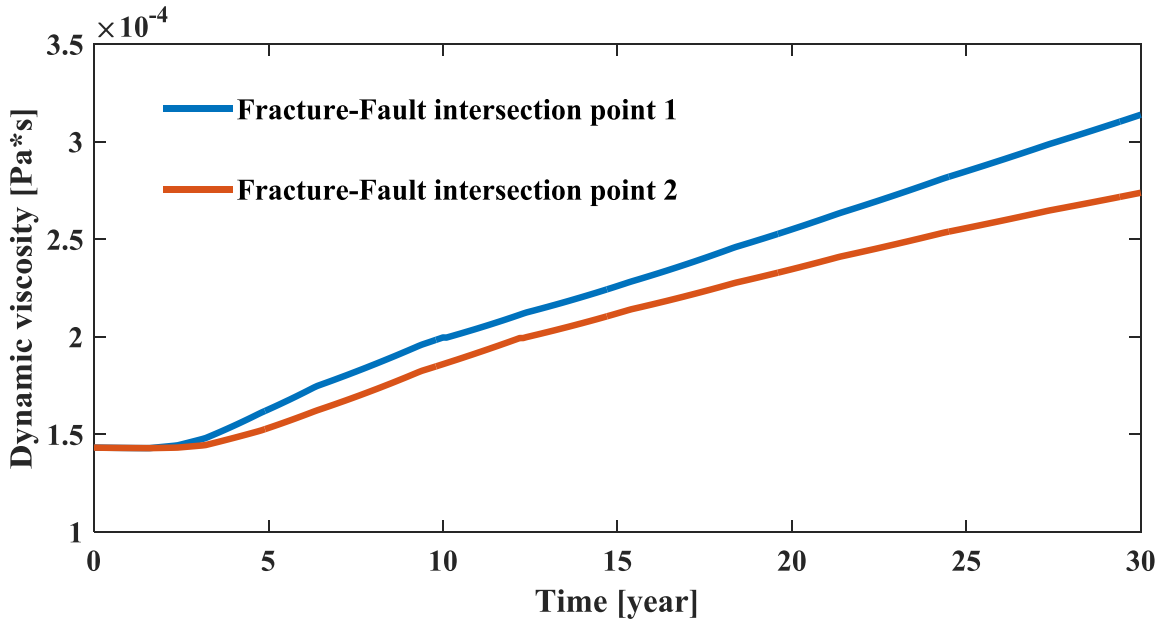

Figure 7: Dynamic viscosity profile at fracture-fault intersection points

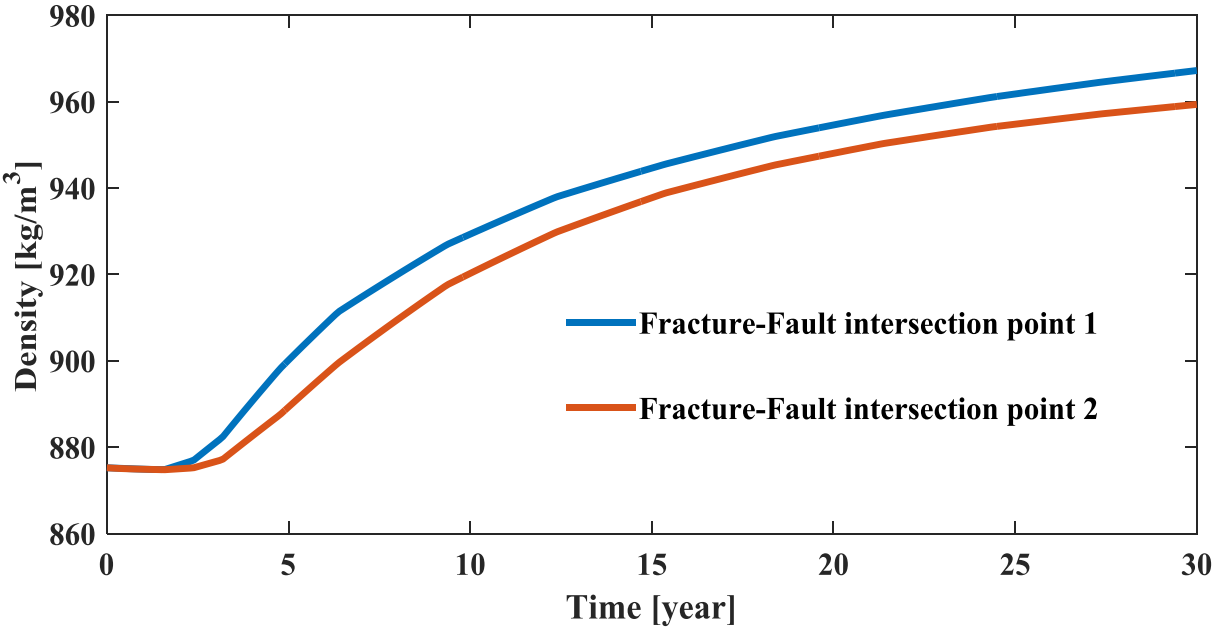

Figure 8: Density profile at fracture-fault intersection points

In the third set, the results were streamlined for both surface temperature and pressure using the heat flux and Darcy's velocity field. Figures 9 and 10 present the results in 3-D, with the streamlines and arrow volumes showing the heat, velocity, and flow direction during simulations. Figures 9a-d display the surface temperature and streamlines for the heat flux, with arrows showing the flow direction. The results are shown for different simulation periods at intervals of 10 years starting from 1 year. It is evident from the results that the heat flows faster through structures with higher permeability such as faults and fractures than the matrix as vividly seen in Figures 9a-d. Likewise, the cold water propagation, in this case the flow initiates from the fracture connected to the injection well, passes through the faults, and the faults finally transmit it to the fracture attached to the production well.

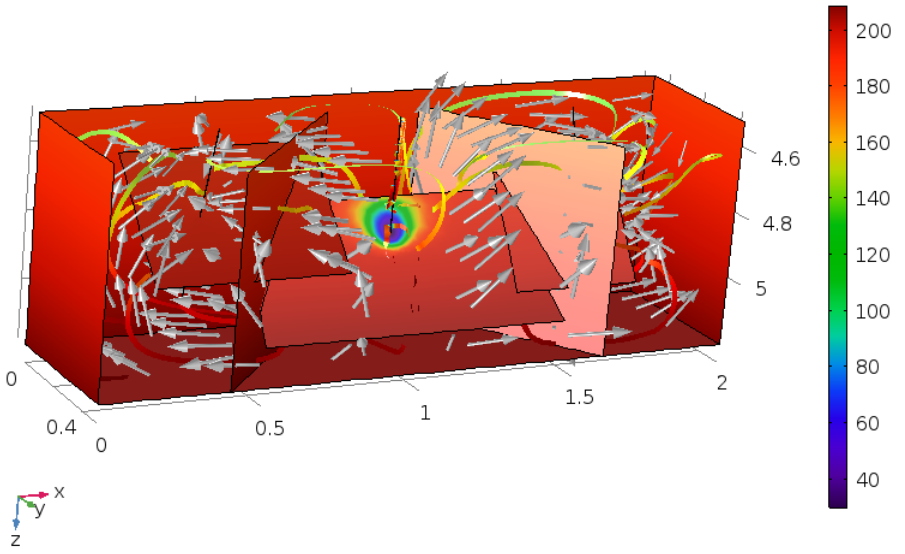

Figure 9a: Surface temperature (°C) and streamline heat flux with arrow volume at 1 year

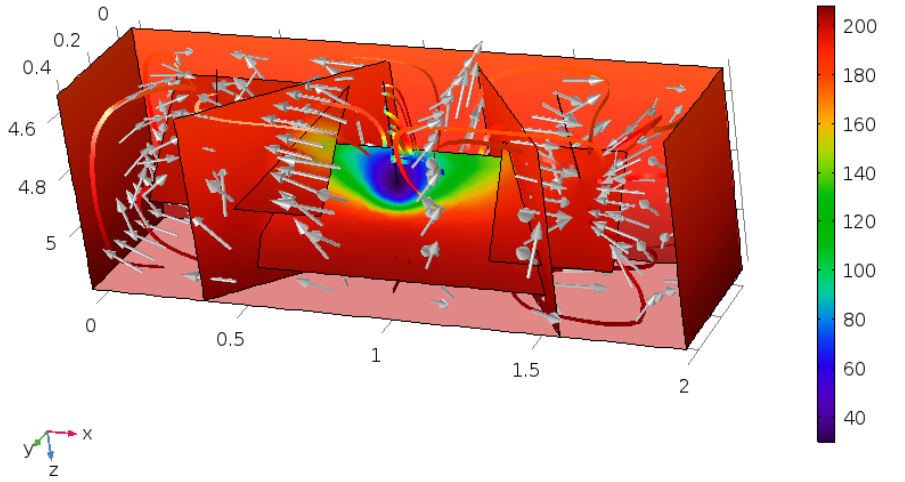

Figure 9b: Surface temperature (°C) and streamline heat flux with arrow volume at 10 years

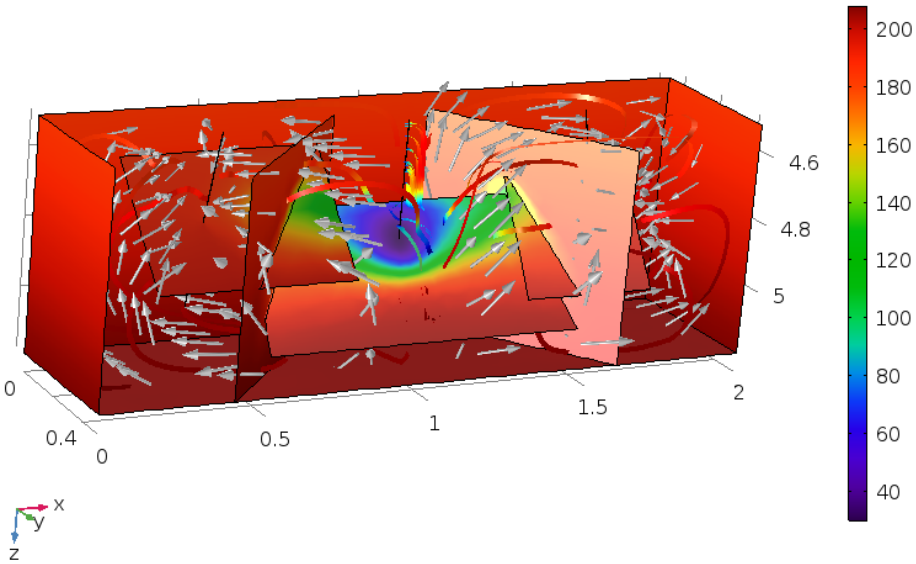

Fig. 9c: Surface temperature (°C) and streamline heat flux with arrow volume at 20 years

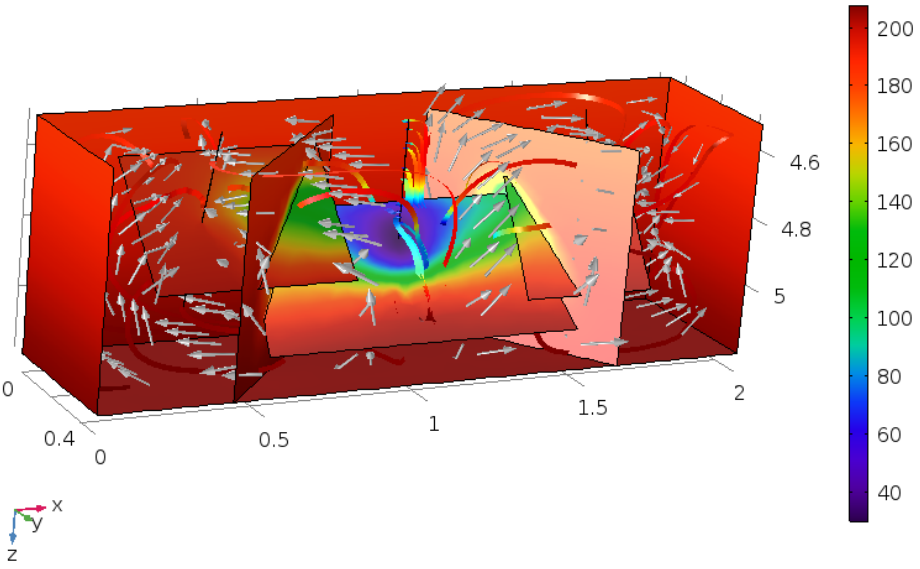

Figure 9d: Surface temperature (°C) and streamline heat flux with arrow volume at 30 years

Figure 9: Surface temperature (°C) and streamline heat flux with arrow volume at several simulation stages

Figures 10a-d presents the surface pressure with streamlines and arrows for Darcy's velocity field at different simulation stages. The stages reported here include 1, 10, 20, and 30 years' simulation periods. The arrows and streamlines indicate the flow velocity directions with changes as the pressure decreases in the neighbouring matrix and the surrounding faults, while at the injection wellbore a constant pressure boundary conditions are applied that make it impossible to decline at the fracture surface.

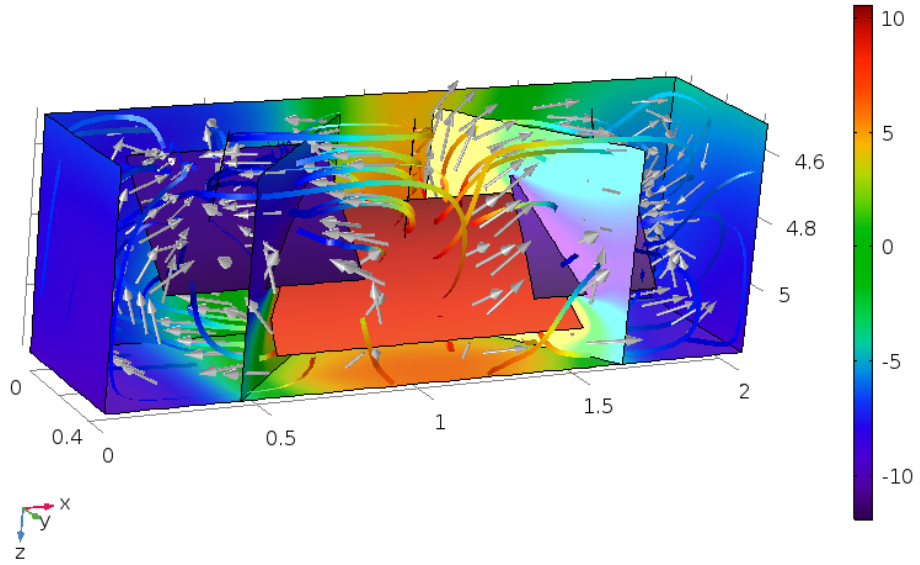

Figure 10a: Surface pressure (MPa) and streamline Darcy's velocity field with arrows at 1 year

5. CONCLUSION

In this study, a numerical model of a triple porosity-permeability model is developed using a computationally efficient finite element method for coupled transient fluid and heat transport in a deep geothermal system. The thermal and fluid interaction between the fractures, faults, the matrix, and the wellbore components are explicitly included in the numerical model, allowing the reduction of the spatial discretization from 3D to 1D and making the model highly efficient. In this study, three sets of results are analysed; the first round of the results is concerned with temperature and enthalpy breakthrough curves at the production wellhead under the simulation period of 30 years. As expected, after 4.8 years of simulation, a decline in the breakthrough curve from that 4.8-year simulated period gradually continues until the end of the simulation for both parameters.

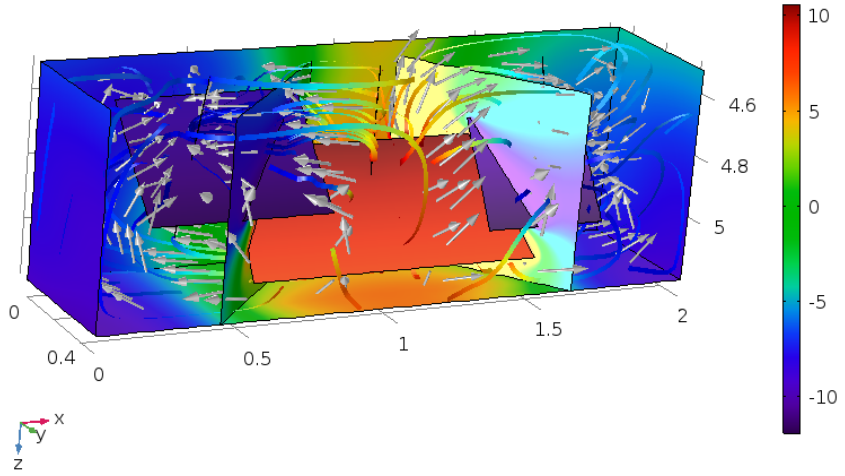

Figure 10b: Surface pressure (MPa) and streamline Darcy's velocity field with arrows at 10 years

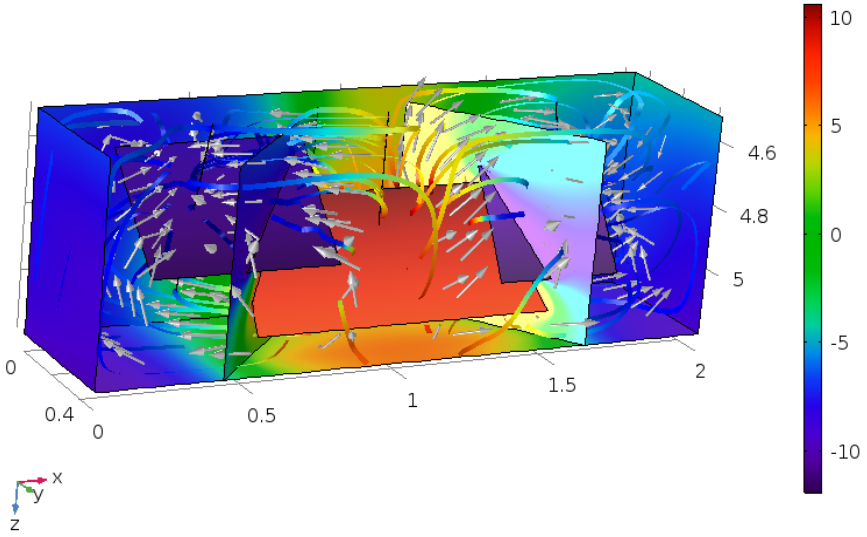

Figure 10c: Surface pressure (MPa) and streamline Darcy's velocity field with arrows at 20 years

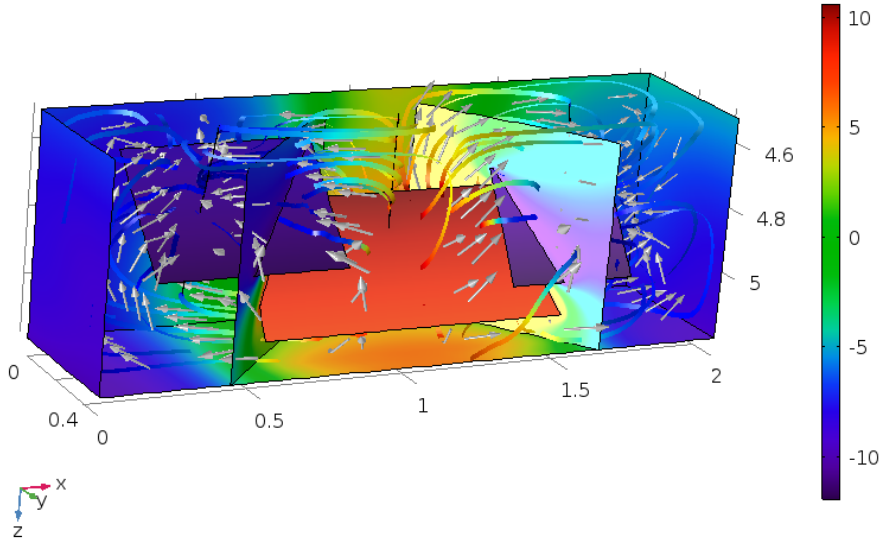

Figure 10d: Surface pressure (MPa) and streamline Darcy's velocity field with arrows at 30 years

Figure 10: Surface pressure (MPa) and streamline Darcy's velocity field with arrow at several simulation stages

The second sets of the results present the pressure, temperature, dynamic viscosity, and density at the fracture-fault intersection points as presented in the paper. In the third sets, the results, streamlined for both heat flux and Darcy's velocity field, are examined for temperature and pressure. The results are presented in 3D with the streamlines and arrow volumes showing the heat, velocity, and flow direction during simulations. As a consequence of the computational capability and precision, the proposed numerical model provides the means for more insight into modelling naturally fractured reservoirs with multiple pore media that might assist in improving the approaches used for capturing realistic reservoir behaviour in the long term.

ACKNOWLEDGEMENT

The first author acknowledges the PhD scholarship funding support earned from both the University of Greenwich (UK) and the Petroleum Technology Development Fund (PTDF) (Nigeria).

REFERENCES

Aliyu, M.D. & Chen, H., 2016. Numerical Modelling of Coupled Hydro-Thermal Processes of the Soultz Heterogeneous Geothermal System. In *ECCOMAS Congress 2016 VII European Congress on Computational Methods in Applied Sciences and Engineering M. Papadrakakis, V. Papadopoulos, G. Stefanou, V. Plevris (eds.) Crete Island, Greece, 5–10 June 2016*. Crete Island, Greece, pp. 1–13.

Aliyu, M.D., Chen, H. & Harireche, O., 2016. Finite element modelling for productivity of geothermal reservoirs via extraction well. In *Proceedings of the 24th UK Conference of the Association for Computational Mechanics in Engineering 31 March– 01 April 2016, Cardiff University, Cardiff*. Cardiff, pp. 331–334.

Altmann, J.B. et al., 2014. Pore pressure stress coupling in 3D and consequences for reservoir stress states and fault reactivation. *Geothermics*, 52, pp.195–205.

Baria, R. et al., 1999. HDR/HWR reservoirs: Concepts, understanding and creation. *Geothermics*, 28(4–5), pp.533–552.

Bower, K.M. & Zyvoloski, G., 1997. A numerical model for thermo-hydro-mechanical coupling in fractured rock. *International Journal of Rock Mechanics and Mining Sciences*, 34(8), pp.1201–1211.

Choi, E.S., Cheema, T. & Islam, M.R., 1997. A new dual-porosity/dual-permeability model with non-Darcian flow through fractures. *Journal of Petroleum Science and Engineering*, 17(3–4), pp.331–344.

Genter, A. et al., 2010. Contribution of the exploration of deep crystalline fractured reservoir of Soultz to the knowledge of enhanced geothermal systems (EGS). *Comptes Rendus Geoscience*, 342(7–8), pp.502–516.

Genter, A. et al., 2009. The EGS Soultz project (France): From reservoir development to electricity production. *Transactions - Geothermal Resources Council*, 33(October), pp.346–351.

Gérard, A. et al., 2006. The deep EGS (Enhanced Geothermal System) project at Soultz-sous-Forêts (Alsace, France). *Geothermics*, 35(5–6), pp.473–483.

Guillou-Frottier, L. et al., 2013. Structure of hydrothermal convection in the Upper Rhine Graben as inferred from corrected temperature data and basin-scale numerical models. *Journal of Volcanology and Geothermal Research*, 256(July 2016), pp.29–49.

Izadi, G. & Elsworth, D., 2015. The influence of thermal-hydraulic-mechanical- and chemical effects on the evolution of permeability, seismicity and heat production in geothermal reservoirs. *Geothermics*, 53, pp.385–395.

Jaime Jemuel C. Austria, J. & Sullivan, M.J.O., 2015. Dual Porosity Models of a Two-phase Geothermal Reservoir. In *World Geothermal Congress 2015 Melbourne, Australia, 19-25 April 2015*. Melbourne, pp. 1–2.

Jain, C., Vogt, C. & Clauser, C., 2015. Maximum potential for geothermal power in Germany based on engineered geothermal systems. *Geothermal Energy*, 3(1), p.15.

Kolditz, O., 1995a. Modelling flow and heat transfer in fractured rocks: Conceptual model of a 3-D deterministic fracture network. *Geothermics*, 24(3), pp.451–470.

Kolditz, O., 1995b. Modelling flow and heat transfer in fractured rocks: dimensional effect of matrix heat diffusion. *Geothermics*, 24(3), pp.421–437.

Lim, K.T. & Aziz, K., 1995. Matrix-fracture transfer shape factors for dual-porosity simulators. *Journal of Petroleum Science and Engineering*, 13(3–4), pp.169–178.

Mohan, A.R. et al., 2015. Modeling the CO2-based enhanced geothermal system (EGS) paired with integrated gasification combined cycle (IGCC) for symbiotic integration of carbon dioxide sequestration with geothermal heat utilization. *International Journal of Greenhouse Gas Control*, 32, pp.197–212.

Nie, R.-S. et al., 2012. Dual Porosity and Dual Permeability Modeling of Horizontal Well in Naturally Fractured Reservoir. *Transport in Porous Media*, 92(1), pp.213–235.

Pribnow, D. & Clauser, C., 2000. Heat and fluid flow at the Soultz hot dry rock system in the Rhine Graben. In *World Geothermal Congress, Kyushu-Tohoku, Japan*. Kyushu-Tohoku, Japan, pp. 3835–3840.

Ranjbar, E. & Hassanzadeh, H., 2011. Matrix–fracture transfer shape factor for modeling flow of a compressible fluid in dual-porosity media. *Advances in Water Resources*, 34(5), pp.627–639.

Schumacher, M.E., 2002. Upper Rhine Graben: Role of preexisting structures during rift evolution. *Tectonics*, 21(1), pp.6–17.

Suirez-Arriaga, M.-Cc., 2002. Tetra-Porosity Models of Geothermal Reservoirs with Faults. *Geothermal Resources Council Transactions*, 26(September 22-25), pp.847–852.

Wang, S. et al., 2015. A Numerical Study of the Thermal-Mechanical Behaviors of Fractured Geothermal Reservoirs. In *Fortieth Workshop on Geothermal Reservoir Engineering Stanford University, Stanford, California, January 26-28, 2015*. California, pp. 1–15.

Zimmerman, R.W. et al., 1993. A numerical dual-porosity model with semianalytical treatment of fracture/matrix flow. *Water Resources Research*, 29(7), pp.2127–2137.